

# Risk assessment for slope monitoring

Yin Zhang<sup>1,\*</sup> and Ingo Neumann<sup>1</sup>

<sup>1</sup> Geodetic Institute, Leibniz Universität Hannover

**Abstract.** One main goal of geodetic deformation monitoring and analysis is minimizing the risk of unexpected collapses of artificial objects and geologic hazards. Nowadays, the methodology in applied geodesy and mathematically founded decisions are usually based on probabilities and significance levels but not on the risk (consequences or costs) itself.

In this study, a new concept which is based on the utility theory is introduced to the current methodology. It allows the consideration of consequences or costs for geodetic decision making in order to meet the real requirements. In this case, possible decisions are evaluated with cost functions for type I and II errors. Finally, the decision leading to the minimum costs or consequences is chosen as the most beneficial one. This procedure allows also identifying the most beneficial additional measurements to reduce the risk of an individual monitoring process. In the last part, the theoretical concept is applied to an example in slope monitoring.

**Keywords.** geodetic monitoring, hypothesis testing, utility theory, cost functions, decision making.

## 1 Introduction

### 1.1 General introduction

One main goal of geodetic deformation monitoring and analysis is minimizing the risk of unexpected collapses of artificial objects and geologic hazards. Nowadays, the methodology in applied geodesy and mathematically founded decisions are usually based on probabilities and significance levels but not on the risk (consequences or costs) itself.

In the classical case, hypothesis testing in linear models is applied [8] to decide about a critical behavior of e.g. a slide slope. The two possible results of the test are the acceptance or the rejection of the predefined hypotheses, which are typically called null (stable slope) and alternative hypothesis (moving slope or not stable slope), respectively.

**Corresponding author:** Yin Zhang, Geodetic Institute, Leibniz Universität Hannover, Nienburger Straße 1, D-30167 Hannover, Germany. E-mail: zhang@gih.uni-hannover.de.

Received: July 26, 2012. Accepted: March 07, 2013.

The choice of the null or alternative hypothesis is based on probabilities only, which have more or less no reference to practical applications. For instance, when the same probabilities under acceptance or rejection region appear, wrong decisions can be made and each decision may lead to dramatically different consequences.

A suitable way to consider consequences within the decision process is the so called "utility theory" in decision making (e.g. [1]). It allows the consideration of consequences or costs for geodetic decision making in order to meet the real requirements. In this case, possible decisions are evaluated with cost functions for type I and II errors. Finally, the decision leading to the minimum costs or consequences is chosen as the most beneficial one. This procedure allows also identifying the most beneficial additional measurements to reduce the risk of an individual monitoring process.

In our specific research, we assess the risks with regard to the consequences or costs for responding or avoiding the real damages on facilities or people in case of a slide slope. According to common sense, costs of false decisions are higher than for correct ones. Therefore, the corresponding occurring damages which may happen in case of a false decision are more expensive than for the correct ones.

The new concept considered in decision making will be mathematically introduced in Section 3, after a short overview in Section 2 for basic information of hypothesis testing. The general procedure using a new concept for the geodetic measurement processes will be given in Section 4. In the last section, the theoretical concept is applied to a practical example in slope monitoring, and the obtained results are discussed. Finally, the paper is concluded and an outlook is given.

### 1.2 Background information of the monitoring project Hornbergl

In order to interpret the approach on a practical manner, the slide slope monitoring project of Hornbergl is taken as an example in this paper.

The mountain "Hornbergl" (see Figure 1) has an altitude of 1755 meters and is located near Reutte, Tyrol (Austria). On the south mountain slope, there is an area named "Luag ins Land" covered with massive fissures and crevices. Due to its specific geological formation, excessive rainfall or sudden thaw both may cause unstable slides. During the last 20 years, periodically geodetic surveys were arranged for monitoring the slide slope in this area so as to avoid fatal risks or hazards. For more information concerning this monitoring process see [3] or [6].



**Figure 1.** Overview of Hornbergl and area "Luag ins Land".

Figure 2 shows the distribution of monitoring points and its relative position to the town in the valley which is marked with a pink ellipse. It can be found that most monitoring points are located close to each other in the left-middle of the figure, except P5, P6 and P9. These three points are located far from the town and also far from the ridge where most other monitoring points are located around. More detailed information of each monitoring point will be discussed later in Section 5.2.

### 1.3 Monitoring data

The Cartesian coordinate frame used in GPS describes the location of a GPS user or satellite with three dimensional coordinates: X, Y and Z, which are generally called ECEF coordinates (Earth-Centered, Earth-Fixed), see e.g. [10]. The GPS data used for this study is only available at specific epochs, and has accuracies of several millimeter. Due to the situation that the time gap between these static GPS epochs is large, the idea is to combine GPS data with tachymeter data which can be measured during the time gap (between GPS-epochs). In this case, the conversion of the GPS data to a local based coordinate system is required.

The use of a reference ellipsoid allows the conversion of the ECEF coordinates to the more commonly used geodetic coordinates of Latitude, Longitude, and Altitude, it can then be converted to a second map reference which interprets small regions in a two dimensional flat surface. The coordinates of the reference frame are transformed to the Bessel ellipsoid which fits especially well to the geoid curvature of Europe and Eurasia. The method used in this paper refers to [15], pp 99-102.

Next, the projection to the Gauß-Krüger Coordinate System (3 degree strip) needs to be implemented. Due to its complicated procedure, it won't be discussed in this paper and for more detailed information of coordinate systems' transformation and map projection, please refer to [4] or [11]. The use of a local flat coordinate system shall be sufficient for the paper due to the relatively small area and to focus on the analysis procedure in case of utility values.

Strictly, a joint 3D-adjustment of GPS and terrestrial data is required.

The next step is to transform the polar tachymeter data onto the same coordinate system for the sake of data combination. The required additional observations which are observed by a tachymeter between the time gaps of the GPS epochs are the horizontal direction (Hz), vertical angle (V) and slope distance (S).

The computation for slope distance and horizontal direction just follows the geometrical laws of two spacial points. For the determination of the vertical angle, the earth's curvature and the refraction correction need to be considered. We model the relationship between V and Z with equation (12.19a) in [5] p. 454.

For every step of the calculations above, the general law of variance-covariance propagation described in mathematical form as

$$\Sigma_{\mathbf{Y}\mathbf{Y}} = \mathbf{A}\Sigma_{\mathbf{X}\mathbf{X}}\mathbf{A}^T \quad (1)$$

with  $\mathbf{Y} = f(\mathbf{X})$  is applied. The values in  $\mathbf{Y}$  are a function of the values in  $\mathbf{X}$ , and the coefficient matrix  $\mathbf{A}$  is determined by the derivative  $\frac{\partial f}{\partial \mathbf{X}}$  of the function with respect to  $\mathbf{X}$ .  $\Sigma_{\mathbf{X}\mathbf{X}}$  is the variance matrix for the values in  $\mathbf{X}$ , and  $\Sigma_{\mathbf{Y}\mathbf{Y}}$  is the variance matrix of the resulting variables in  $\mathbf{Y}$ . For a nonlinear set of equations, it should be linearized first using Taylor's theorem, and the matrix  $\mathbf{A}$  is the so called Jacobian matrix [2].

## 2 Basic information of hypothesis testing

As mentioned in previous section, the methodology in geodetic deformation monitoring for minimizing the risk of unexpected collapses of artificial objects and geologic hazards are mathematically founded on base of probabilities and significance levels nowadays. Generally, decision making can be regarded as a process resulting in a selection from any number of alternatives. However, for the sake of simplicity, the classical case of decision making in geodesy is hypothesis testing treated with only two alternatives: acceptance or rejection of the null hypothesis.

According to [8], the unknown parameters  $\theta$  span the parameter space  $B$ , thus  $\theta \in B$ . Then a statistical hypothesis test is defined as the assumption that a parameter vector  $\theta$  belongs to the subset  $b$  of the parameter space  $B$  ( $b \subset B$ ) or to its complement  $B \setminus b$ , thus,  $\theta \in b$  or  $\theta \in B \setminus b$ . The assumption  $H_0$  with  $\theta \in b$  is called null hypothesis and the assumption  $H_1$  with  $\theta \in B \setminus b$  is called alternative hypothesis.

Four possible situations can occur when a decision is made (shown in Table 1), among them are two incorrect decisions well known as Type I and Type II errors.

Based on the observations  $\mathbf{y}$ , a test statistic  $T = f(\mathbf{y})$  is introduced as a function of  $\mathbf{y}$ . The null hypothesis is accepted, if the test statistic  $T$  belongs to the subspace  $S_A$



Figure 2. Overview of monitoring points.

Situations	Decisions	
	Acceptance of $H_0$	Rejection of $H_0$
$H_0$ is true	Correct choice of the null hypothesis	Incorrect choice of the alternative hypothesis ( <b>Type I error</b> )
$H_0$ is false ( $H_1$ is true)	Incorrect choice of the null hypothesis ( <b>Type II error</b> )	Correct choice of the alternative hypothesis

Table 1. Possible situations within the test decision.

of the probability space of the observations, the acceptance region. Otherwise, the null hypothesis is rejected, if the test statistic  $T$  belongs to the subspace  $S_R$ , the rejection or critical region.

The regions of acceptance  $A$  and rejection  $R$  are classical sets in  $\theta \in \mathfrak{R}^U$ , and they can be modeled by indicator functions as

$$i_A(\theta) = \begin{cases} 1, & \text{if } \theta \in b \\ 0, & \text{else} \end{cases} \quad (2)$$

$$i_R(\theta) = \begin{cases} 1, & \text{if } \theta \in B \setminus b \\ 0, & \text{else.} \end{cases}$$

The indicator functions  $i_A(\theta)$  and  $i_R(\theta)$  denote the region of acceptance and the region of rejection, respectively. Usually, the region of acceptance  $A$  for the null hypothesis and its indicator function  $i_A$  can be seen as a mapping on the parameter space  $i_A : B \rightarrow \{0; 1\}$ :

$$A := \{x, i_A(x) | x \in \mathfrak{R}\} \quad (3)$$

with  $i_A : \mathfrak{R}^u \rightarrow \{0; 1\}$  and  $x \in \mathfrak{R}$

And it is obviously known that the two indicator functions are complementary to each other, thus,  $i_R(\theta) = 1 - i_A(\theta)$ :

$$R := \{x, i_R(x) = 1 - i_A(x) | x \in \mathfrak{R}\} \quad (4)$$

with  $i_A : \mathfrak{R}^u \rightarrow \{0; 1\}$  and  $x \in \mathfrak{R}$

For the determination of lower and upper bounds of the indicator functions, it depends on the combined optimization of Type I and Type II errors on the subsets  $S_A$  and  $S_R$  of the probability space of observations.

In hypothesis testing on geodesy, it is typical to map multiple dimensional tests onto one dimension space. Hence, the study of this paper follows the same way, assuming the final decision of test can be carried out in one dimension space. This general mapping procedure is introduced in Section 4.

Then the test value  $T = f(y)$  is compared with the acceptance and rejection regions, on which the final decision is based. In Figure 3, it shows one example of such hypothesis testing. In this example, the test accepts the null hypothesis.

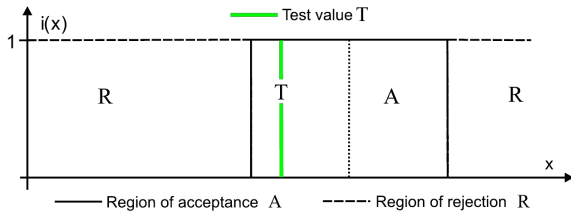


**Figure 3.** Classical case of hypothesis testing with acceptance and rejection regions [13].

### 3 Making decision with cost functions

#### 3.1 Utility theory

In decision making, the simplest case is that the situations resulting from each of these decisions are known exactly, and the preferred one can be decided just through simple comparisons. But the general case is that often we can only predict the probabilities of different situations. One reasonable description of human decision making comes from the utility theory, the main idea behind it is to judge each possible decision with a utility value. Therefore, when the same probabilities under acceptance or rejection region appear, wrong decisions and possible dramatically different consequences can be avoided.

To describe the overall effect of a decision, two special situations: a very beneficial situation  $S_1$  and a very bad situation  $S_0$  are chosen. Assuming that there is a "lottery"  $L(p)$  equivalent to the situation  $S_1$  occurring with probability  $p$   $p \in [0, 1]$ , and  $S_0$  with a probability  $1 - p$ , then for every situation  $S_i$  with a probability of  $p_i$  in between  $S_0$  and  $S_1$ , there exists a probability  $U_i$  for which  $S_i$  is equivalent to the lottery  $L(U_i)$ . This value  $U_i$  is called the utility of the situation  $S_i$ . For each decision of  $d_i$ , the consequences of it are equivalent to a composite lottery  $L$ . And every situation  $S_{ij}$  has a probability  $p_{ij}$  which leads to a lottery  $L(U_j)$ . As the outcomes of each lottery  $L(U_j)$  are  $S_{0j}$  and  $S_{1j}$ , the composite  $L$  also get either  $S_{0j}$  or  $S_{1j}$ . The expected utilities of each decision  $d$  can be interpreted as [9]:

$$K_i = \sum_{j=1}^n p_{ij} \cdot U_j \quad (5)$$

According to Section 2, there are four utility values corresponding to the possible situations, respectively:

- $U_{00}$ : utility for a correct choice of the null hypothesis;
- $U_{01}$ : utility for a incorrect choice of the alternative hypothesis (Type I error);
- $U_{11}$ : utility for a correct choice of the alternative hypothesis;
- $U_{10}$ : utility for a incorrect choice of the null hypothesis (Type II error).

And considering that the correct decision is always better than the incorrect one, it can be derived that  $U_{00} > U_{10}$  and  $U_{11} > U_{01}$ .

Suppose we have a steel part for a machine and we need to decide based on its length whether the steel part is suitable to be used in the machine or not. Assuming the standard length of 50 mm with a lower and upper threshold between 49 and 51 mm we must decide whether it is suitable for use, or it may also destroy the machine slowly and cause more risk later. In this case, if we make a decision that the part is unsuitable (costs for  $U_{11}$  or  $U_{01}$ ), then we abandon it and buy a new part; on the other hand, if we classify it as suitable (costs for  $U_{10}$  or  $U_{00}$ ), the machine may be destroyed little by little and costs are much higher for the reparation. Therefore, we make a decision based on the expected utilities which allows us to find the decision with the minimum costs.

More examples will be given in Section 5.2. For more information and examples of utility theory, please refer to e.g. [9].

#### 3.2 Decisions for regulatory thresholds

It is known that a reasonable approach of decision making comes with the aid of utility theory, and it needs to select between one of several decisions. The simplest case is that the exact consequences of each decision are known, and then the decision making can be as simple as comparing these situations and deciding a preferable one. However, the general case is that situations are not always explicit, and in practice, often only the probabilities of different situations can be predicted.

Assuming that  $\rho_0(T)$  and  $\rho_1(T)$  are probability densities of  $T$  for objects satisfying the null and the alternative hypotheses, respectively. The probability  $p_0(T) = P(H_0|T)$  for a test value  $T$  which satisfies the null hypothesis can be determined using Bayes' Theorem [7]:

$$\begin{aligned} p_0(T) &= \frac{P(T|H_0) \cdot P(H_0)}{P(T|H_0) \cdot P(H_0) + P(T|H_1) \cdot P(H_1)} \\ &= \frac{\rho_0(T) \cdot P(H_0)}{\rho_0(T) \cdot P(H_0) + \rho_1(T) \cdot P(H_1)} \end{aligned} \quad (6)$$

where  $P(H_0)$  and  $P(H_1)$  stand for the probabilities for a randomly chosen object satisfying null or alternative hypothesis.

Alternatively, the probability  $p_1(T) = P(H_1|T)$  that  $T$  satisfies the alternative hypothesis can be determined as

$$p_1(T) = 1 - \frac{\rho_0(T) \cdot P(H_0)}{\rho_0(T) \cdot P(H_0) + \rho_1(T) \cdot P(H_1)} = 1 - p_0(T) \quad (7)$$

In the next step, according to [9], the expected utilities of null and alternative hypotheses,  $K_0$  and  $K_1$ , can be calcu-

lated with the aid of probabilities and utility values

$$\begin{aligned} K_0 &= p_0(T)U_{00} + p_1(T)U_{10} = p_0(T)(U_{00} - U_{10}) + U_{10} \\ K_1 &= p_0(T)U_{01} + p_1(T)U_{11} = p_0(T)(U_{01} - U_{11}) + U_{11} \end{aligned} \quad (8)$$

Since a final decision is selected resulting in the largest expected utility (the minimum costs) of the hypothesis, the null hypothesis is chosen if

$$p_0(T)U_{00} + p_1(T)U_{10} \geq p_0(T)U_{01} + p_1(T)U_{11} \quad (9)$$

holds. As mentioned in Section 3.1,  $U_{00} > U_{01}$  and  $U_{11} > U_{10}$ , then the equation (9) can be simplified and written as

$$\frac{p_0(T)}{p_1(T)} \geq \frac{U_{11} - U_{10}}{U_{00} - U_{01}} \quad (10)$$

Substituting the Bayes-Equation (6), it leads to

$$\frac{\rho_0(T)}{\rho_1(T)} \geq r_0 = \frac{(U_{11} - U_{10})p_1(T)}{(U_{00} - U_{01})p_0(T)} \quad (11)$$

When the right hand side of equation (11) is known, the decision is made by comparing with the existing threshold  $r_0$ . Then, the so called Neyman-Pearson criterion can be summarized as following:

- the null hypothesis is selected, if  $\frac{\rho_0(T)}{\rho_1(T)} \geq r_0$  holds,
- otherwise, the alternative hypothesis is selected, if  $\frac{\rho_0(T)}{\rho_1(T)} < r_0$  holds.

Regulatory thresholds for critical movements of a slope play a key role in monitoring concept nowadays. When tolerances are given, a production or inspection process can be checked by measurements with deviation detection between the actual dimension and the nominal dimension of an object. The nominal dimension is defined by lower and upper bounds which are known as regulatory thresholds.

Through equations (8), equation (9) can also be written as

$$p_0(T)(U_{00} - U_{10}) + U_{10} \geq p_0(T)(U_{01} - U_{11}) + U_{11} \quad (12)$$

Then, the rearranged form is

$$p_0(T) \geq p_{0,\text{critical}} = \frac{U_{11} - U_{10}}{U_{00} - U_{10} - U_{01} + U_{11}} \quad (13)$$

The null hypothesis is selected, if the probability  $p_0(T)$  is larger or equal than the critical probability  $p_{0,\text{critical}}$ . The regions of acceptance  $A$  and rejection  $R$  are defined by the indicator functions (see Section 2), and the probabilities of  $p_0(T)$  and  $p_1(T)$  meaning the test value  $T$  belongs to acceptance region  $A$  or rejection region  $R$

are computed following:

$$\begin{aligned} p_0(T) &= \int_A \rho_T(x) dx \\ p_1(T) &= 1 - \int_A \rho_T(x) dx \end{aligned} \quad (14)$$

The decisions for regular thresholds discussed above can also be extended to the linguistic imprecision or fuzziness of the formulated hypotheses, when it deals with reasoning more approximate rather than fixed and exact. It leads to the definition of regions of transition between strict acceptance and rejection of a given hypothesis. Furthermore, it is also possible to consider non-stochastic uncertainties, such as systematic measurement errors. For more information of the strategy for non-stochastic measurement uncertainties and linguistic uncertainty for regulatory thresholds, it is referred to [12] and [14].

#### 4 General procedure for steering of measurement process with cost functions

The test statistic is computed based on the observations  $T = f(\mathbf{y})$ . However, since there are not enough monitoring objects (e.g. slide slopes) to construct a reasonable pdf in geodesy, the distribution of objects is not known normally, and the hypothesis is formulated based on the observations.

These two distributions of the null hypothesis and the alternative hypothesis could be attributed to observations that contain only random errors versus observations containing blunders. Then the distribution of the test statistics under the null hypothesis can be known, but the pdf of the test statistics under the alternative hypothesis is not exactly specified.

According to [13], the pdf of the test statistic under null hypothesis is assumed as  $T_{H_0} \sim \rho_{T,H_0}(x, \lambda = 0)$  with a non-centrality parameter  $\lambda = 0$ . When the assumption of the null hypothesis is prevailing, the alternative hypothesis can be formulated as the negation of the null hypothesis, and the pdf of the test static under alternative hypothesis follows the same structure as  $T_{H_1} \sim \rho_{T,H_1}(x, \lambda \neq 0)$  with a non-centrality parameter  $\lambda \neq 0$ . The concept described here can be applied to the case of a general linear hypothesis within a Gauss-Markoff model, and the slide slope monitoring of Hornbergl as an example will be discussed in Section 5.

The hypotheses based on the parameter in the linear models can be therefore formulated as a linear combination of the parameters. With the matrix  $\mathbf{C}$  and the vector  $\mathbf{w}$ , the null hypothesis can be notated as [8]:

$$H_0 : \mathbf{C}\boldsymbol{\beta} = \mathbf{w} \quad (15)$$

and the alternative hypothesis as:

$$H_1 : \mathbf{C}\boldsymbol{\beta} = \bar{\mathbf{w}} \neq \mathbf{w} \quad (16)$$

The non-centrality parameter of the pdf  $\rho_{T,H_1}(x, \lambda \neq 0)$  can be computed with the aid of the expected changes of the parameter under the null hypothesis:

$$\lambda = \boldsymbol{\varphi}(\bar{\mathbf{w}} - \mathbf{w}) \quad (17)$$

In case of linear hypothesis, we obtain the test value  $T$  according to [8]:

$$T = \frac{1}{r\hat{\sigma}^2} (\mathbf{C}\boldsymbol{\beta} - \mathbf{w})^T \left[ \mathbf{C} (\mathbf{A}^T \mathbf{A})^{-1} \mathbf{C}^T \right]^+ (\mathbf{C}\boldsymbol{\beta} - \mathbf{w}) \quad (18)$$

with  $\mathbf{A}$  is the Jacobi (design) matrix of the estimation,  $-\hat{\sigma}^2$  is the posteriori variance factor and  $\left[ \mathbf{C} (\mathbf{A}^T \mathbf{A})^{-1} \mathbf{C}^T \right]^+$  is the pseudo-inverse due to rank deficiencies. In this circumstance, the rank deficiencies are defined by the linear dependent columns of  $\mathbf{C}$  on the premise that the column regular matrix  $\mathbf{A}$  has a full rank. In reality, the matrix  $\mathbf{A}$  is not always full rank; however, we simplified the problem to focus more on utilities in this paper. The test statistic  $T$  follows a central ( $\lambda = 0$ ) Fisher distribution  $F$  for the null hypothesis:

$$T_{H_0} \sim F(r, f, \lambda = 0) \quad (19)$$

and  $r = rg \left[ \mathbf{C} (\mathbf{A}^T \mathbf{A})^{-1} \mathbf{C}^T \right]^+$  stands for the number of linear independent combinations of the tested parameters, as well as  $f$  stands for the degree of freedom of the estimation. Hence, under the alternative hypothesis, the test static follows a non-central ( $\lambda \neq 0$ ) Fisher distribution  $F'$ :

$$T_{H_1} \sim F'(r, f, \lambda) \quad (20)$$

with

$$\lambda = \frac{1}{\sigma^2} (\bar{\mathbf{w}} - \mathbf{w})^T \left[ \mathbf{C} (\mathbf{A}^T \mathbf{A})^{-1} \mathbf{C}^T \right]^+ (\bar{\mathbf{w}} - \mathbf{w}) \quad (21)$$

The general procedure of steering the measurement process with consideration of cost functions is based on a loop obeying the following steps:

- Define the changes in parameters:  $d\mathbf{w} = \bar{\mathbf{w}} - \mathbf{w}$ .
- Determine the non-centrality parameter for the test statistic under the alternative hypothesis with equations (17) or (21).
- Calculate the probabilities  $p_0(T)$  and  $p_1(T)$  using equations (14) under the assumption of  $P(H_0) = P(H_1)$ .
- Calculate the expected total utilities of  $K_0$  and  $K_1$  using equation (8).

- Make the decision according to equation (12) or (13) for regulatory thresholds.

It shows that the function of the test decision depends on the changes in the parameter with respect to the utility values of each decision. The more expensive a type II error in comparison to the type I error, the earlier the null hypothesis is rejected. This is equivalent to the conclusion that more risk (costs) may appear. In the next section, an example for the methodology is discussed in detail.

## 5 Geodetic monitoring of the slide slope Hornbergl

### 5.1 Risk decrease with the aid of additional observation

In this section, the example of monitoring the slide slope Hornbergl is discussed. The general information of Hornbergl and the distribution of monitoring points were introduced in Section 1.2.

In order to decrease the risk and the negative environmental impacts, the monitoring of the slope is carried out with both GPS data and tachymeter data. The analysed GPS measurements give monitoring data in specific frequency, before the GPS data of the next epoch will be available, the tachymeter will give additional observations according to the last decision with consideration of cost functions. The aim is to detect and to decide about significant movements by analysing the risk or the consequence that may occur.

As mentioned in Section 1.3, all the GPS data was mapped to a flat surface: Gauß-Krüger Coordinate System before the data combination process. For convenience of interpretation, the "GPS data" mentioned in the following are all referring to the transformed data form. Then, the possible shifts of monitoring points between every two GPS epochs can be calculated through the transformed coordinates data directly, but when taking additional measurements observed by tachymeter into account, we need to transform every set of coordinate data X, Y and Z to observations of slope distance, horizontal angle and vertical angle, assuming that a tachymeter observes the specific monitoring point from the stand point. The type of tachymeter chosen here is a *Leica* TM 30, the standard deviation for distance observation is 1 mm + 0.6 ppm and for angle observation (observed in 2 faces) 0.15 mgon.

The combination of GPS and terrestrial observations can be carried out by transforming the local control coordinates into GNSS reference datum, or by transforming the GNSS points into the local datum. For example, the Helmert transformation is the most rigorous method of converting between reference frames. In this paper, we choose the other way to transform the GPS coordinates into 2D Cartesian coordinates through the map projection approach. This method is especially useful when the local coordinates are in some arbitrarily created temporal coordinate system. In

this project, the transformation was chosen since the interpretation of the results in the Cartesian coordinate system is better than in a spacial one. For further information of two transformation approaches, please refer to Ghilani [2]. In this example, the GPS data of the very first epoch is taken as a reference, and all the following monitoring data are compared with the reference. Then, the whole procedure for risk decrease with the aid of additional observation in Hornbergl executes the following loop:

1. Read the GPS data of the coming epoch and calculate the distance differences between the current epoch and the reference, as well as the standard deviations of them.
2. Calculate the shifts for all monitoring points, which is defined by the point-to-point distance between current epoch and the reference epoch:

$$\Delta \text{def}_i = \sqrt{(x_i - x_{r,i}^0)^2 + (y_i - y_{r,i}^0)^2 + (z_i - z_{r,i}^0)^2} \quad (22)$$

where  $\Delta \text{def}_i$  stands for the current shift computed for the  $i$ -th monitoring point, while  $x_{r,i}^0$ ,  $y_{r,i}^0$  and  $z_{r,i}^0$  are the coordinates of the reference epoch for the  $i$ -th monitoring point  $x_i$ ,  $y_i$  and  $z_i$  denote the coordinates of the  $i$ -th monitoring point at current epoch.

The standard deviations  $\sigma^2 \Delta \text{def}_i$  of shifts are computed under the law of error propagation (Section 1.3):

$$\sigma^2 \Delta \text{def}_i = \begin{bmatrix} \frac{\partial \Delta \text{def}_i}{\partial x_i} & \frac{\partial \Delta \text{def}_i}{\partial x_{r,i}^0} & \dots & \frac{\partial \Delta \text{def}_i}{\partial z_{r,i}^0} \end{bmatrix} \times \begin{bmatrix} \sigma_{x_i}^2 & \sigma_{x_i, x_{r,i}^0} & \dots & \sigma_{x_i, z_{r,i}^0} \\ \sigma_{x_{r,i}^0, x_i} & \sigma_{x_{r,i}^0}^2 & \dots & \sigma_{x_{r,i}^0, z_{r,i}^0} \\ \vdots & \vdots & \ddots & \vdots \\ \sigma_{z_{r,i}^0, x_i} & \sigma_{z_{r,i}^0, x_{r,i}^0} & \dots & \sigma_{z_{r,i}^0}^2 \end{bmatrix} \begin{bmatrix} \frac{\partial \Delta \text{def}_i}{\partial x_i} \\ \frac{\partial \Delta \text{def}_i}{\partial x_{r,i}^0} \\ \vdots \\ \frac{\partial \Delta \text{def}_i}{\partial z_{r,i}^0} \end{bmatrix} \quad (23)$$

According to the general form of a linear hypothesis from equations (15) and (16), the matrices and vectors are given as

$$\begin{aligned} \mathbf{w} &= 0 \\ \mathbf{C} &= \left[ \frac{\partial \Delta \text{def}_i}{\partial \beta} \right] \\ \beta &= \left[ x_i \quad x_{r,i}^0 \quad y_i \quad y_{r,i}^0 \quad z_i \quad z_{r,i}^0 \quad \dots \right]^T \end{aligned} \quad (24)$$

3. With the help of shifts and their standard deviations, calculate the utility values  $K_0$  and  $K_1$  for every monitoring point using equation (8). The probabilities of  $p_0(T)$  and  $p_1(T)$  meaning the test value  $T$  belongs to acceptance region  $A$  or rejection region  $R$  are computed according to equation (14) with the intuitive thresholds.

4. Choose the more beneficial one from the utility values of  $K_0$  and  $K_1$  as the cost at current epoch for each monitoring point.
5. Check whether the GPS data at next epoch is available. If yes, repeat the above steps 1. to 4. If not, the tachymeter will do the additional measurement during the gap time.

As we expect, the tachymeter observes only one monitoring point as an additional measurement each time. Which point should be chosen to benefit most within the monitoring procedure and reduce the total risk is the question to be answered in the next step.

6. Simulate the tachymeter observations for every monitoring point through the latest GPS data as additional observations.
7. Add the additional observation data to the latest transformed observation data, and estimate the monitoring points using Weighted Least Squares method.
8. With the results of the last step, repeat steps 2., 3. and 4., and compare the new costs with the latest costs (can be the costs either at GPS epoch or at additional measurement epoch).
9. Pick out the point whose cost changed most from the last epoch as an additional measurement. Observe this point with tachymeter and repeat the steps 7. and 8.
10. Go back to step 5. and continue until the end of the procedure.

The slope monitoring procedure works following the steps in a loop as above until the end that neither GPS nor tachymeter data is available or required any more. The working result of the procedure is given in the following section, together with the comparison and analysis between the approaches.

## 5.2 Comparison of two different approaches

In this section, results of two different approaches are given and analysed. They are:

- (i) Risk minimization through accuracy;
- (ii) Minimization of cost functions for  $H_0/H_1$ .

In the following paragraphs, the first approach is concerned. And minimizing risk through accuracy means that only the standard deviations of shifts of the monitoring points are considered. This approach is only presented to show the difference when applying utility values in approach 2. The results are given in Table 2.

As shown in Table 2, the additional tachymeter observations measure the point whose standard deviation of shift decreases most. The geometry relationship between the

Epoch	Procedure and results
<b>GPS_2006</b>	Reference coordinates.
<b>GPS_2007</b>	Standard deviations of shifts: $\sigma\Delta\text{def}_{2007}^0$
Tachymeter measurement 1	The chosen point: P22; $\Delta(\sigma\Delta\text{def})_1 = \sigma\Delta\text{def}_{2007}^0 - \sigma\Delta\text{def}_{2007}^1 = 1.15\text{mm}$
Tachymeter measurement 2	The chosen point: P21; $\Delta(\sigma\Delta\text{def})_2 = \sigma\Delta\text{def}_{2007}^1 - \sigma\Delta\text{def}_{2007}^2 = 1.12\text{ mm}$
Tachymeter measurement 3	The chosen point: P23; $\Delta(\sigma\Delta\text{def})_3 = \sigma\Delta\text{def}_{2007}^2 - \sigma\Delta\text{def}_{2007}^3 = 1.11\text{ mm}$
<b>GPS_2009</b>	Standard deviations of shifts: $\sigma\Delta\text{def}_{2009}^0$
Tachymeter measurement 1	The chosen point: P5; $\Delta(\sigma\Delta\text{def})_1 = \sigma\Delta\text{def}_{2009}^0 - \sigma\Delta\text{def}_{2009}^1 = 2.25\text{mm}$
Tachymeter measurement 2	The chosen point: P26; $\Delta(\sigma\Delta\text{def})_2 = \sigma\Delta\text{def}_{2009}^1 - \sigma\Delta\text{def}_{2009}^2 = 1.16\text{ mm}$
Tachymeter measurement 3	The chosen point: P22; $\Delta(\sigma\Delta\text{def})_3 = \sigma\Delta\text{def}_{2009}^2 - \sigma\Delta\text{def}_{2009}^3 = 1.12\text{ mm}$
Tachymeter measurement 4	The chosen point: W2; $\Delta(\sigma\Delta\text{def})_4 = \sigma\Delta\text{def}_{2009}^3 - \sigma\Delta\text{def}_{2009}^4 = 1.11\text{ mm}$
Tachymeter measurement 5	The chosen point: P9; $\Delta(\sigma\Delta\text{def})_5 = \sigma\Delta\text{def}_{2009}^4 - \sigma\Delta\text{def}_{2009}^5 = 1.10\text{ mm}$
<b>GPS_2010</b>	Standard deviations of shifts: $\sigma\Delta\text{def}_{2010}^0$
Tachymeter measurement 1	The chosen point: P5; $\Delta(\sigma\Delta\text{def})_1 = \sigma\Delta\text{def}_{2010}^0 - \sigma\Delta\text{def}_{2010}^1 = 3.60\text{ mm}$
Tachymeter measurement 2	The chosen point: P9; $\Delta(\sigma\Delta\text{def})_2 = \sigma\Delta\text{def}_{2010}^1 - \sigma\Delta\text{def}_{2010}^2 = 1.14\text{ mm}$
Tachymeter measurement 3	The chosen point: P26; $\Delta(\sigma\Delta\text{def})_3 = \sigma\Delta\text{def}_{2010}^2 - \sigma\Delta\text{def}_{2010}^3 = 1.04\text{mm}$

**Table 2.** Monitoring results (approach 1).

Point No.	Location	Possible damage in case of a landslide
P1	near skiing field	facilities, people
P2	near the trench	dams, buildings, farmlands
P21	near the trench	dams, buildings, farmlands
P22	other side of the valley	small rivers
P23	near the trench	dams, buildings, farmlands
P26	near the trench	dams, buildings, farmlands
P27	other side of the valley	small rivers
P5	far from town	small rivers
P6	far from town	small rivers
P9	far from town	small rivers
W1	near skiing field	facilities, people
W2	near the trench	dams, buildings, farmlands

**Table 3.** Information of monitoring points.



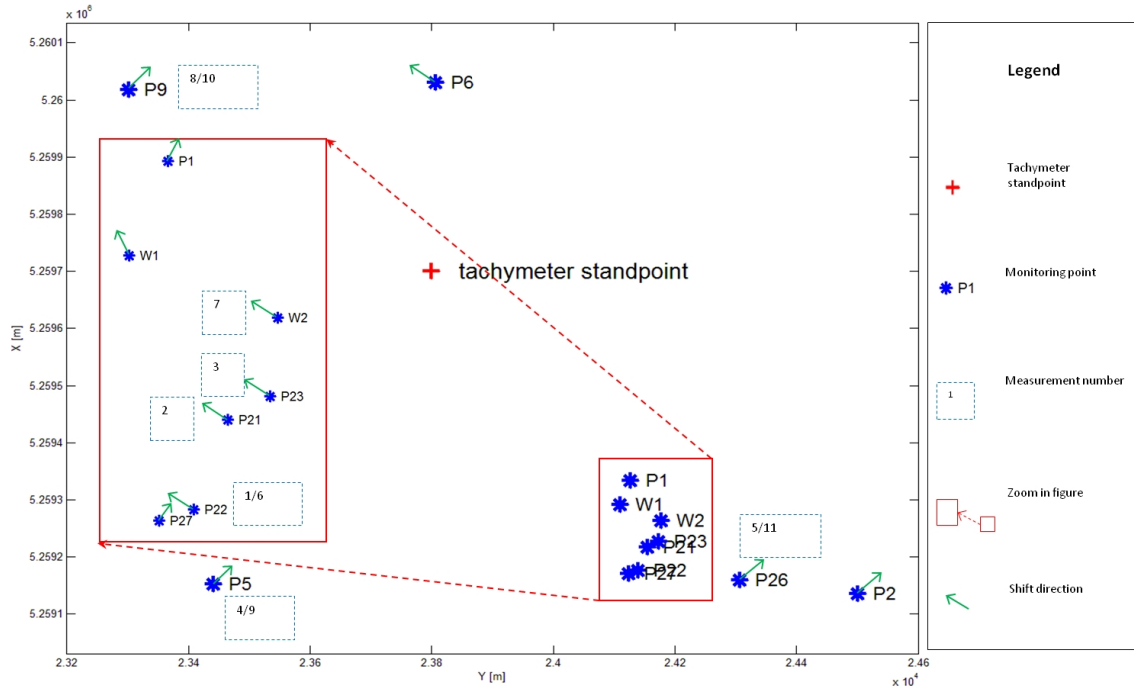


Figure 4. Top view of monitoring points with marked additional observations (approach 1).

tachymeter stand point and the monitoring points can be viewed from Figure 4.

Figure 4 shows a top view of all monitoring points with indications of shift direction, a zoom-in figure and the numbers of additional measurements showed in blue dashed rectangles. It interprets the topological relationship between each point, however, since there is no elevation information contained, the distance from the tachymeter standpoint to each monitoring point is not absolutely as it shows in Figure 4. Consider the slope distances observed by tachymeter, the distances between standpoint and monitoring points are divided into three types due to the length, as shown below:

- Short distance: P6, P1, W1;
- Middle distance: W2, P21, P23, P27, P22;
- Long distance: P9, P5, P26; P2.

In this approach, the monitoring points P5, P9, P22 and P26 were chosen two times, respectively, to be measured additionally in order to reduce the standard deviation of shift by the greatest extent. As the additional measurements are observed by the same tachymeter at the same standpoint, the accuracies of the observations mostly depend on the distance from the standpoint to the monitoring point. But the GPS data have different standard deviations of coordinates, which have no relation with the slope distances. Therefore, the choices are influenced by several factors. But after analysing the standard deviation of GPS data for all the points, it is found that the most chosen points have

bigger standard deviations generally. And the distances from the tachymeter standpoint to the most chosen points are not short.

In the second approach, besides the movements of monitoring points, the costs of real risks are taken into consideration. According to Section 3.1, the assessment of risks is based on the utility values of four different situations. In order to determine the utility values more reasonable, we need to analyse the locations of monitoring points first.

Figure 5 shows a zoom-in photo taken from the direction backing on the town in valley. The middle part of the figure marked with a red ellipse shows the trench of mountain slope which connects the town in valley. Many monitoring points are located near this area, and are a good indicator for a collapse of the slide slope. In the extended area, there are several small dams which are built to absorb a large amount of rainfall or thaw. Further considering the connection between this area and the town, those dams, farmlands and buildings may be damaged or destroyed if landslides happen in the area of these points (shown in Table 3). In the area marked with a blue ellipse on the left side of Figure 5, possible collapses can only damage small rivers since the artificial constructions are far away from it. On the right side, it locates a skiing field marked with a yellow ellipse, and significant risks can be caused if collapses happen on e.g. P1 and W1, where hazards may occur to artificial facilities or people.

The detailed information of locations and related possible damages are shown in Table 3. Magnitude of damage

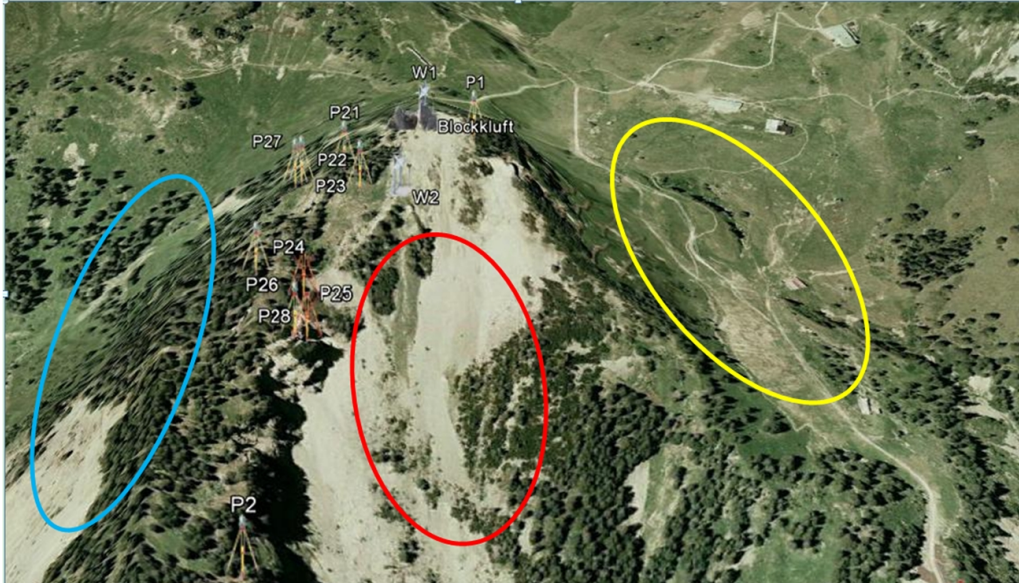


Figure 5. Surroundings of monitoring points.

related to each monitoring point is determined partly based on it. In the meanwhile, the utility values are determined also according to Section 3.1. It is known that  $U_{00} > U_{10}$ , and  $U_{11} > U_{01}$ , furthermore,  $U_{11}$ : the utility for a correct choice of the alternative hypothesis costs less than it for a incorrect choice:  $U_{10}$ . In this specific project, the meaning of each utility value is:

- $U_{00}$ : utility for correctly classifying the monitoring point as a stable type;
- $U_{01}$  : utility for incorrectly classifying the monitoring point as an unstable type;
- $U_{11}$ : utility for correctly classifying the monitoring point as an unstable type;
- $U_{10}$ : utility for incorrectly classifying the monitoring point as a stable type.

In Table 4, the utility values for all monitoring points are given. The thresholds are determined intuitively according to their locations and the geological formation. Within one of the next papers, the determination of the thresholds and their influence on the decision results will be discussed more in detail.

The monitoring procedure and its results are displayed in Table 5. As the focus of this approach is to minimize the risks, the monitoring point chosen to make additional observation is the one whose costs change mostly after estimation with the additional measurements. In Table 5, the amounts of costs that changed are given.

In this case, the most chosen monitoring points P1 and P9 are chosen three times. Following them, the point P6 was chosen two times as additional observed point. The dis-

Point No.	P1	P9	P26
Threshold [mm]	50	50	10
$\Delta\text{def}_{2007}^0$ [mm]	44.64	10.34	93.73
$\sigma\Delta\text{def}_{2007}^0$ [mm]	10.14	4.54	13.75
$\Delta\text{def}_{2009}^0$ [mm]	52.51	21.59	336.91
$\sigma\Delta\text{def}_{2009}^0$ [mm]	10.30	13.10	15.12
$\Delta\text{def}_{2010}^0$ [mm]	74.05	21.56	413.63
$\sigma\Delta\text{def}_{2010}^0$ [mm]	11.32	12.65	14.96

Table 6. Relationship between the thresholds and the distance differences of GPS data.

tribution of all monitoring points and their additional measurements are shown in Figure 6.

The results of this approach are determined together by the accuracies of input data, distances from standpoint to the monitoring points and their specific thresholds and utility values as well. In Table 6, it shows the relationship between the thresholds and the distance differences of GPS data for some typical monitoring points. And for the convenience of expression, the above introduced abbreviations are used in the table.

Known from previous sections, the adjustment procedure with (simulated) additional measurement gives the same or very similar results for distance difference ( $\Delta\text{def}$ ) of this monitoring point but a smaller standard deviation  $\sigma\Delta\text{def}$ . In this case, when  $\Delta\text{def}$  is located only inside the acceptance region or far away from it, even if the standard deviation of it gets smaller, the distribution of  $\Delta\text{def}$  (obey normal distribution in this paper) is still mainly inside the acceptance region or outside it as the situation without additional mea-

Point No.	Threshold	U <sub>00</sub>	U <sub>01</sub>	U <sub>11</sub>	U <sub>10</sub>
	[mm]				
P1	50	1000	25000	15000	150000
P2	50	1000	35000	25000	250000
P21	100	1000	35000	25000	250000
P22	100	1000	15000	10000	50000
P23	100	1000	35000	25000	250000
P26	10	1000	35000	25000	250000
P27	10	1000	15000	10000	50000
P5	10	1000	15000	10000	50000
P6	50	1000	15000	10000	50000
P9	50	1000	15000	10000	50000
W1	50	1000	25000	15000	150000
W2	10	1000	35000	25000	250000

Table 4. Utility values of monitoring points (approach 2).

Epoch	Procedure and Results
<b>GPS_2006</b>	Reference coordinates.
<b>GPS_2007</b>	$K_{2007}^0 = \min\{K_0, K_1\}$
Tachymeter measurement 1	The chosen point: P22; $\Delta K = K_{2007}^0 - K_{2007}^1 = 1092.74$
Tachymeter measurement 2	The chosen point: P9; $\Delta K = K_{2007}^1 - K_{2007}^2 = 214.41$
Tachymeter measurement 3	The chosen point: P1; $\Delta K = K_{2007}^2 - K_{2007}^3 = -201.11$
<b>GPS_2009</b>	$K_{2009}^0 = \min\{K_0, K_1\}$
Tachymeter measurement 1	The chosen point: P9; $\Delta K = K_{2009}^0 - K_{2009}^1 = 1033.20$
Tachymeter measurement 2	The chosen point: P6; $\Delta K = K_{2009}^1 - K_{2009}^2 = 141.85$
Tachymeter measurement 3	The chosen point: P1; $\Delta K = K_{2009}^2 - K_{2009}^3 = 84.86$
Tachymeter measurement 4	The chosen point: P2; $\Delta K = K_{2009}^3 - K_{2009}^4 = 63.10$
Tachymeter measurement 5	The chosen point: P5; $\Delta K = K_{2009}^4 - K_{2009}^5 = 27.29$
<b>GPS_2010</b>	$K_{2010}^0 = \min\{K_0, K_1\}$
Tachymeter measurement 1	The chosen point: P9; $\Delta K = K_{2010}^0 - K_{2010}^1 = 1017.85$
Tachymeter measurement 2	The chosen point: P6; $\Delta K = K_{2010}^1 - K_{2010}^2 = 764.90$
Tachymeter measurement 3	The chosen point: P1; $\Delta K = K_{2010}^2 - K_{2010}^3 = 68.10$

Table 5. Monitoring results (approach 2).

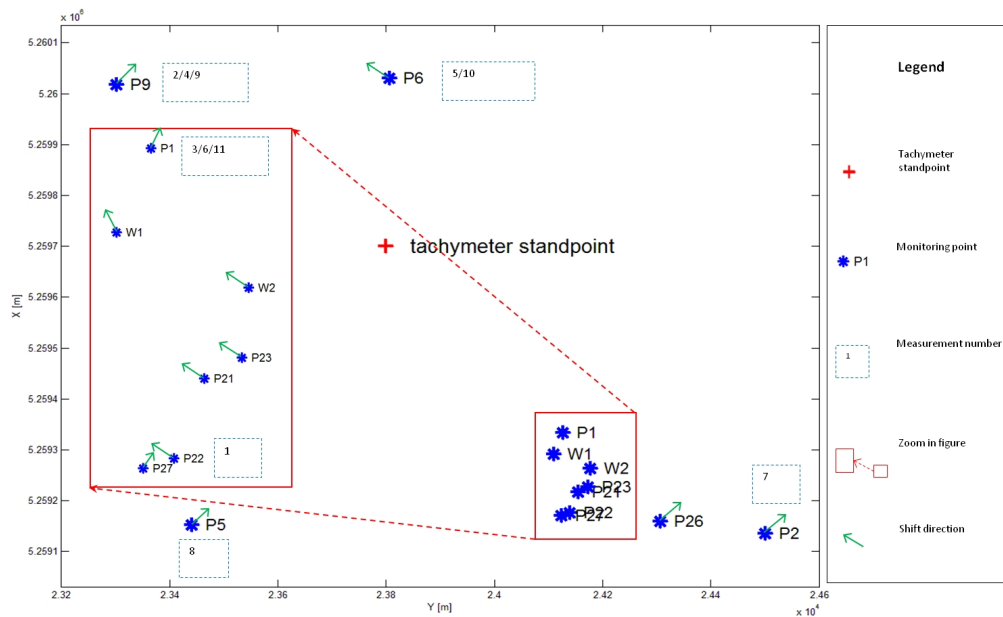


**Figure 6.** Top view of monitoring points with marked additional observations (approach 2).

surement. It can be good interpreted by the example of P26 in Table 6. On the other hand, when the value  $\Delta_{\text{def}}$  is close to the threshold, the probability of  $\Delta_{\text{def}}$  located inside or outside the acceptance region may change a lot and then leads to big decrease of costs generally.

In Table 5, there is an especial result giving an increasing cost after the third additional measurement for GPS data in 2007. According to Table 6, the  $\Delta_{\text{def}}$  value is located closely on the left side of the threshold. With the (simulated) additional measurement, the adjustment procedure gives smaller standard deviation but the same distance difference, which means the probability  $p_0(T)$  getting larger. Then it is easy to draw the conclusion with the help of equation (8), that  $K_0$  gets smaller and  $K_1$  gets larger. Because of the very expensive utility values for incorrect choices,  $K_1$  was chosen with and without additional measurement. Therefore, it gives a negative cost difference.

However, the costs were expected to decrease always with additional measurements. The further study of changing trend of cost function and the relationship between costs and the distribution of distance difference will be considered and presented in future research.

## 6 Conclusion and outlook

The geodetic monitoring concepts have to be more accurate and reliable when more risks or costs act on the assumption of a moving slide slope or on a collapse of a construction. However, the current geodetic monitoring makes decisions without the consideration of costs or risks themselves;

therefore they are not optimal for collapses of neither artificial objects nor geologic hazards.

This paper shows a concept in decision making of the consideration of costs or consequences with the aid of "utility theory". The decisions are evaluated extending the statistical hypothesis tests with cost functions for type I and II errors. And finally, it leads to the minimum costs or consequences chosen as the most beneficial one in order to reduce the risk of an individual monitoring process.

This strategy presented in the paper steers the measurement process optimally by identifying the most beneficial measurement for the monitoring project. And the particular importance of it is that it allows different types of measurement data combined together for estimation and optimization of a monitoring process.

In future, the concept and approach shall be extended to multiple criteria decisions with more than two alternatives, deal with more approximate rather than fixed and exact thresholds and define the regions of transition between strict acceptance and rejection of a given hypothesis. Additionally, it is also meaningful to implement the strategy in a real project to numerically analyse and optimise the measurement process with respect to consequences.

## Acknowledgments

The presented paper shows results and new ideas developed during the research project NE 1453/3-1 "Steering and optimization of measurement processes in consideration of cost functions", which is funded by the German Research Foundation (DFG). This is gratefully acknowledged by the authors.

## References

- [1] J. Figueira, S. Greco and M. Ehrgott, *Multiple Criteria Decision Analysis: State of the Art Surveys*, International Series in Operations Research & Management Science, Vol. 78, ISBN: 978-0-387-23067-2, 2005
- [2] C. D. Ghilani, *Adjustment Computations: Spatial Data Analysis* (Fifth Edition), John Wiley & Sons, Hoboken - New Jersey, 2010.
- [3] J. Glabsch, O. Heunecke and S. Schuhbäck, Monitoring the Hornbergl Landslide Using a Recently Developed Low Cost GNSS Sensor Network, *J. of Appl. Geodesy* **3** (2009), 179-192.
- [4] E. W. Grafarend and F. W. Krumm, *Map Projections, Cartographic Information Systems*, Springer, Berlin - Heidelberg, 2007.
- [5] H. Kahmen, *Vermessungskunde*, Walter de Gruyter & Co., Berlin, 1997.
- [6] H. Kirschner, *Hornbergl-Bericht zur geologisch-geotechnischen Untersuchung*, Report for Forsttechnischer Dienst of the Wildbach - and Lawinenverbauung, Geological Department Innsbruck, 2006.
- [7] G. J. Klir, *Uncertainty and Information: Foundations of Generalized Information Theory*, John Wiley & Sons, Hoboken - New Jersey, 2006.
- [8] K. R. Koch, *Parameter estimation and hypothesis testing in linear models*, Springer, Berlin - Heidelberg - New York, 1999.
- [9] V. Kreinovich H. T. Nguyen and S. Niwitpong, Statistical Hypothesis Testing Under Interval Uncertainty: An Overview, *Journal of Intelligent Technologies and Applied Statistics*, **1** (2008), 1-33.
- [10] A. Leick, *GPS Satellite Surveying* (3rd Ed.), John Wiley & Sons, Hoboken - New Jersey, 2004.
- [11] D. H. Maling, *Coordinate Systems and Map Projections* (2nd Ed.), Pergamon, Oxford, 1992.
- [12] I. Neumann and H. Kutterer, *Optimal hypothesis testing in case of regulatory thresholds* In: Sneeuw, N.; Novák, P.; Crespi, M.; Sansò, F. (Eds.): Proceedings of the 7th Hotine-Marussi-Symposium, International Association of Geodesy Symposia, Springer, Berlin - New York, Vol. 137 , Part 3, 75-80, DOI: 10.1007/978-3-642-22078-4\_11, 2011.
- [13] I. Neumann and Y. Zhang, *Assessment of risk within geodetic decisions*, Joint International Symposium on Deformation Monitoring, November 2011, Hong Kong, China (CD Proceedings).
- [14] S. Niwitpong, H. T. Nguyen, V. Kreinovich and I. Neumann, Hypothesis testing with interval data: case of regulatory constraints, *International Journal of Intelligent Technology and Applied Statistics* Vol. 1, No. 2 (2008) pp. 19-41.
- [15] W. Torge, *Geodesy* (3rd Edition). Walter de Gruyter & Co., Berlin, 2001.